Epidermal nevus syndrome: MR of intracranial involvement.

S Lazzeri, M Mascalchi, M Cellerini, M G Martinetti and G Dal Pozzo

AJNR Am J Neuroradiol 1993, 14 (5) 1255-1257
http://www.ajnr.org/content/14/5/1255

Epidermal Nevus Syndrome: MR of Intracranial Involvement

Stefania Lazzeri,[1] Mario Mascalchi,[2] Martino Cellerini,[1] Maria Grazia Martinetti,[3] and Giancarlo Dal Pozzo[1]

Summary: Focal thickening of the calvarium, hypoplasia of the white matter, cortical calcifications, and a leptomeningeal drape that enhanced after contrast injection were demonstrated by MR in the parietooccipital region ipsilateral to a facial sebaceous nevus in a patient with epidermal nevus syndrome.

Index terms: Phakomatoses; Brain, occipital lobe; Brain parietal lobe; Brain, magnetic resonance

Epidermal nevus syndrome (ENS), or nevus linearis sebaceous, is a rare congenital neurocutaneous disorder characterized by the association of epidermal nevi of different types with other developmental defects of the central nervous system, eye, and skeleton (1).

Central nervous system anomalies are found predominantly in patients with epidermal nevi on the head and are usually ipsilateral to the skin lesion (2). Mental retardation, seizures, and focal neurologic deficits are the most common clinical features (2).

We found one patient with ENS studied with unenhanced magnetic resonance (MR) imaging reported in the literature (3). Herein we report pre- and postcontrast MR findings with computed tomographic (CT) correlations in a patient with ENS.

Case Report

An 18-year-old woman with a diagnosis of ENS underwent a cranial MR examination at 0.5 T because of transient worsening of a congenital right hemiparesis associated with frontal headache.

At birth clusters of yellow nodules showing granular surfaces pitted with hypertrophic sebaceous glands consistent with Jadassohn sebaceous nevus were present in the left frontomaxillary region of the face; they were associated with alopecia in the left temporoparietal region. A mild right-sided hemiparesis was also noted. Ocular abnormalities included bilateral retinal depigmentation and coloboma of the head of the left optic nerve. A biopsy at 3 months of age confirmed that the facial nevi were the sebaceous type. A febrile convulsion on the right side occurred at 9 months of age, and two generalized seizures occurred when the patient was 2 years old. Neurologic examination at the time of MR revealed hypoplasia of the right side of the body with ipsilateral mild spastic paresis and moderate global mental retardation.

On MR the right cerebral hemisphere was noted to be larger than the left, and there was focal thickening of the left parietal bone (Fig 1A). A subarachnoid cyst at the pole of the left temporal lobe and widening of the left Sylvian fissure were also present (not shown). The white matter of the left parietal and occipital lobes was hypoplastic, with enlargement of the trigone and the occipital horn of the left lateral ventricle (Fig 1A–1F). The overlying cortex was covered by a 0.5- to 1.5-cm-thick "drape" that extended into the posterior interhemispheric and left Sylvian fissures, and whose signal behavior on spin-echo and short-inversion-time inversion-recovery sequences pointed to the presence of both fat and vascular components (Fig 1A–1D). In particular, the latter was suggested by the enhancement of the lesion and of the leptomeningeal spaces adjacent to it (Fig 1F) after intravenous administration of gadopentetate dimeglumine (Shering AG, Berlin, Germany) 0.1 mmol/kg. Cortical calcifications beneath the drape were suspected on low-flip-angle gradient-echo images (Fig 1E) and were confirmed by plain CT (Fig 1G). No signal abnormality of the brain parenchyma was detected on MR.

Conventional angiography of the left carotid and vertebral arteries was performed at another institute and showed hypoplasia of the opercular branches of the left middle cerebral artery and of the terminal branches of the posterior left cerebral artery, which arose from the ipsilateral carotid. Paucity of parenchymatous and venous vessels was observed in the left parietooccipital region. Preferential cortical venous drainage due to impaired flow in the superior longitudinal sinus was also present.

No surgery was performed. On a follow-up MR examination 1 year later, the MR findings were unchanged.

Received June 11, 1992; revision requested August 12, received October 9, and accepted October 23.

[1] Neuroradiologia, Dipartimento di Fisiopatologia Clinica, Universitá di Firenze, 50100 Firenze, Italy.

[2] Present address: Cattedra di Radiodiagnostica, Istituto di Radiologia, Universitá di Pisa, Via Roma 67, 56100 Pisa, Italy. Address reprint requests to Mario Mascalchi, MD.

[3] Cattedra di Neuropsichiatria Infantile, Universitá di Firenze, Firenze, Italy.

AJNR 14:1255–1257, Sep/Oct 1993 0195-6108/93/1405-1255

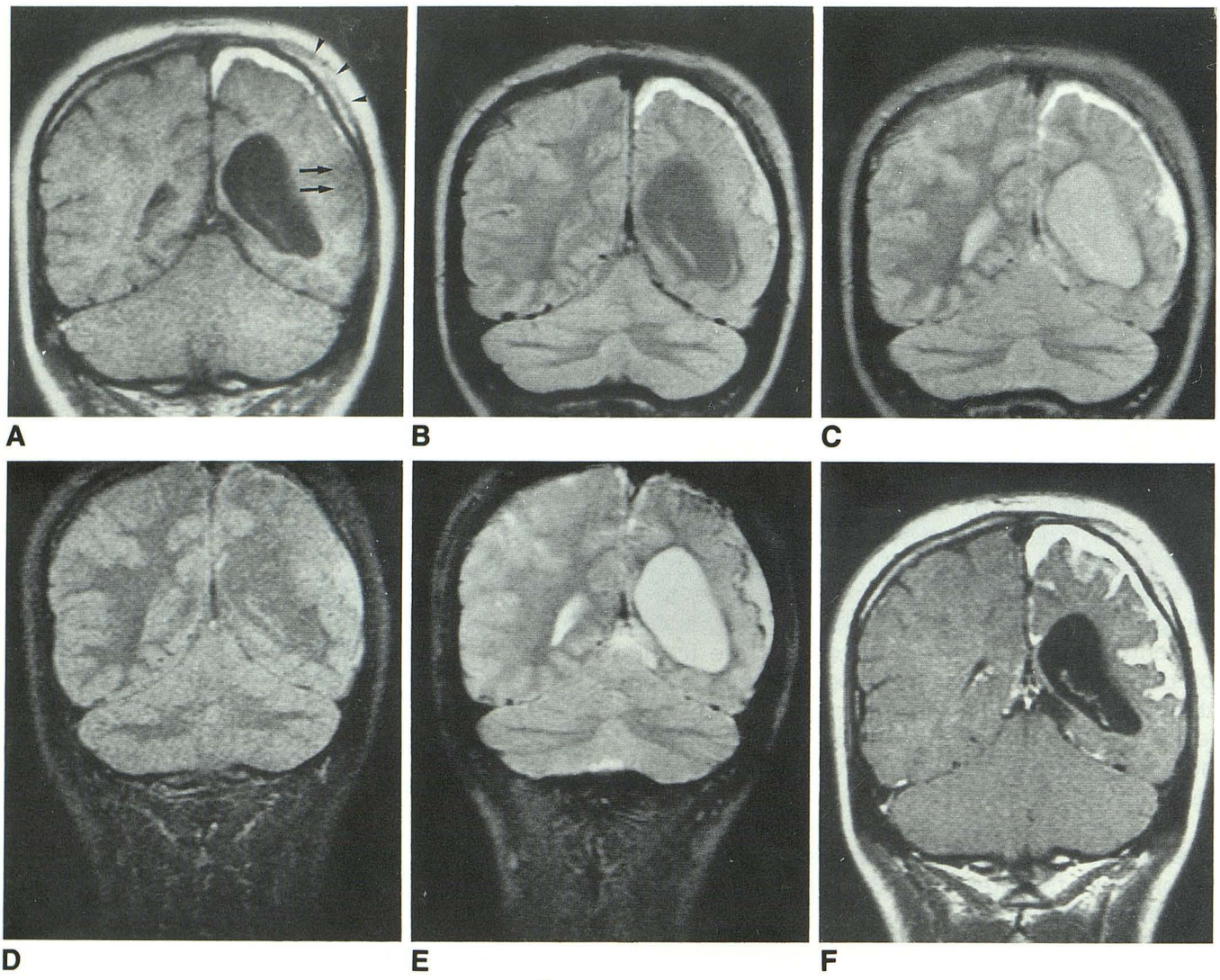

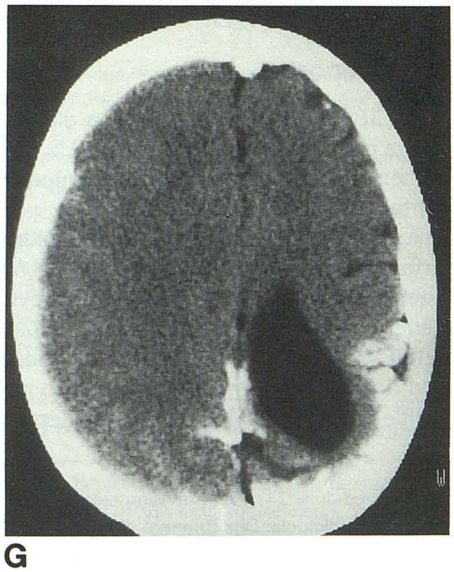

Fig. 1. *A–G*, Coronal T1-weighted (360/30/4) (repetition time/echo time/excitations) spin-echo image (*A*) shows thickening of the left parietal bone (*arrowheads*) and hypoplasia of left parietal and occipital lobes with enlargement of the trigone and occipital horn of the left lateral ventricle. The parietal cortex at the vertex is covered by a 0.5- to 1.5-cm-thick hyperintense drape. An ill-defined hypointensity is appreciable beneath the inferior edge of the abnormal hyperintensity in the temporoparietal region (*black arrows*). On balanced (2240/50) (*B*) and T2-weighted (2240/100) (*C*) coronal spin-echo images the superficial layer of the drape at the vertex shows a progressive decrease of signal intensity similar to that of subcutaneous fat. The signal of this portion almost completely fades on a short-inversion-time inversion-recovery sequence (1220/100/60) (*D*), whereas the portion of the drape near the left Sylvian fissure maintains a high signal intensity. On a low-flip-angle gradient-echo image (15°, 860/45) (*E*) a gyriform rim of low signal intensity is interposed between the inferior portion of the drape and the underlying brain parenchyma. After intravenous administration of gadopentetate dimeglumine (0.1 mmol/kg) a conspicuous enhancement of the leptomeningeal spaces adjacent to the drape spreading into the interhemispheric and left Sylvian fissures is observed on a coronal T1-weighted spin-echo (460/30) image (*F*). Plain CT scan with soft-tissue algorithm (*G*) shows cortical calcifications in the left parieto-occipital regions and bilateral cortical calcifications in the posterior part of the interhemispheric fissure.

Discussion

Very few neuropathologic data are available on structural anomalies of the central nervous system in ENS. They include gliomas, subarachnoid cysts, cortical dysplasia, and leptomeningeal hemangiomas (2).

Conventional x-ray and CT studies have demonstrated cranial and facial asymmetry, focal thickening of the calvarium, cerebral atrophy, dilated ventricles, and cortical calcifications (2). Angiographic studies have revealed poor or increased vascularity of the cortex and subarachnoid spaces under the scalp nevus with arterial dysplasia and nonpatent dural sinuses, aneurysms, and arteriovenous malformations (2). The only MR study we are aware of (3) showed unilateral megalencephaly and white matter hypoplasia associated with pachigyria of the frontal lobe ipsilateral to the nevus.

Thus, the white matter hypoplasia with corresponding dilatation of the lateral ventricle, the asymmetry of the skull with focal thickening of the calvarium, the cortical calcifications, and the temporal subarachnoid cyst observed in our patient are in agreement with prior findings reported in ENS.

Overt changes in the leptomeningeal spaces overlying the affected cerebral hemisphere completed the MR picture in our patient. Because we have no pathologic correlation we can speculate only on the changes underlying these findings.

The hypothesis we submit is that the portions of the drape at the vertex and the one near the Sylvian fissure represent the predominantly sebaceous and vascular components of a leptomeningeal nevus, respectively. The signals of the two portions of the lesion on T1-weighted and short-T1 inversion-recovery images and their behavior after contrast administration support this hypothesis. Histopathologic features of the skin lesion (Jadassohn nevus) in our patient are in agreement with this explanation, because nevus sebaceous is characterized by underdeveloped sebaceous glands (4), and association of epidermal nevi with hamartomatous capillary component has been reported (5, 6).

Undoubtedly, several of the clinical and imaging features in our patient are reminiscent of those typical of the Sturge-Weber (SW) syndrome. However, the type of nevus in our patient was different from that typical of SW syndrome, which is the so-called port-wine nevus (7), and the ocular abnormalities were distinct from SW syndrome in which congenital glaucoma leading to buphthalmos is the usual feature (7). Conversely, the coloboma observed in our patient is typical of ENS (1). From the imaging point of view, hypertrophy of the choroid plexus and prominence of the deep venous system, which are characteristic of SW syndrome were missing in our case (8, 9). Finally, we know of no drape described in patients with the SW syndrome in the MR literature (9–11). On the other hand cerebral hemiatrophy with a parietooccipital distribution and cortical calcifications associated with evidence on postcontrast MR of abnormal meningeal enhancement can be observed in both conditions. The latter feature, however, also has been observed in neurocutaneous melanosis (12) and could be a nonspecific finding common to several neurocutaneous dysplasias. These similarities are not surprising when one recalls that both ENS and SW syndromes are a type of phakomatosis, of which clinical and pathologic overlap is a well-established feature (7).

References

1. Atherton DJ, Rook A. Naevi and other developmental defects. In Rook A, Wilkinson DS, Ebling FJG, Champion RH, Burton JL, eds. *Textbook of dermatology*. 4th ed. Oxford: Blackwell Scientific Publications, 1986:167–227
2. Baker RS, Ross PA, Baumann RJ. Neurologic complications of the epidermal nevus syndrome. *Arch Neurol* 1987;44:227–232
3. Sarwar M, Schafer ME. Brain malformations in linear nevus sebaceous syndrome: an MR study. *J Comput Assist Tomogr* 1988;12:338–340
4. Fizpatrick TB, Eisen AZ, Wolff K, Freedberg IM, Austen KF, eds. *Dermatology in general medicine*. 3rd ed. New York: McGraw-Hill, 1987:787
5. Solomon LM, Fretzin DF, Dewald RL. The epidermal nevus syndrome. *Arch Dermatol* 1968;97:273–285
6. Kuokkanen K, Koivikko M, Alavaikko M. Organoid nevus phakomatosis. *Acta Dermatol Venereol* 1980;60:534–537
7. Adams RD, Victor M. Developmental disease of the nervous system. In: Adams RD, Victor M, eds. *Principles of neurology*. 3rd ed. New York: McGraw-Hill, 1985:902–937
8. Bentson JR, Wilson GH, Newton TH. Cerebral venous drainage pattern of the Sturge-Weber syndrome. *Radiology* 1971;101:111–118
9. Chamberlain MC, Press GA, Hesselink JR. MR imaging and CT in three cases of Sturge-Weber syndrome: prospective comparison. *AJNR: Am J Neuroradiol* 1989;10:491–496
10. Elster AD, Chen MYM. MR imaging of sturge-Weber syndrome: role of gadopentetate dimeglumine and gradient-echo techniques. *AJNR: Am J Neuroradiol* 1990;11:685–689
11. Lipski S, Brunelle F, Aicardi J, Hirsch JF, Lallemand D. Gd-DOTA-enhanced MR imaging in two cases of Sturge-Weber syndrome. *AJNR: Am J Neuroradiol* 1990;11:690–692
12. Rhodes RE, Friedman HS, Hatten HP, Hockenberger B, Oakes WJ, Tomita T. Constrast-enhanced MR imaging of neurocutaneous melanosis. *AJNR: Am J Neuroradiol* 1991;12:380–382